

much information as possible.

- This document may contain data, which exceeds the sheet parameters. It was furnished in this condition by the organizational source and is the best copy available.
- This document may contain tone-on-tone or color graphs, charts and/or pictures, which have been reproduced in black and white.
- This document is paginated as submitted by the original source.
- Portions of this document are not fully legible due to the historical nature of some of the material. However, it is the best reproduction available from the original submission.

NASA TM X-55896

**THE GLOBAL RADIATION BALANCE  
OF THE EARTH ATMOSPHERE SYSTEM  
OBTAINED FROM RADIATION DATA  
OF THE METEOROLOGICAL SATELLITE  
NIMBUS II**

**EHRHARD RASCHKE  
MUSA PASTERNAK**

**AUGUST 1967**



**GODDARD SPACE FLIGHT CENTER  
GREENBELT, MARYLAND**

**N 67-36392**  
(ACCESSION NUMBER)  
**24**  
(PAGES)  
**TMX-55896**  
(NASA CR OR TMX OR AD NUMBER)

FACILITY FORM 602

(THRU)

(CODE)

(CATEGORY)

THE GLOBAL RADIATION BALANCE OF THE EARTH  
ATMOSPHERE SYSTEM OBTAINED FROM RADIATION  
DATA OF THE METEOROLOGICAL  
SATELLITE NIMBUS II

Ehrhard Raschke  
Musa Pasternak  
Laboratory for Atmospheric and  
Biological Sciences

GODDARD SPACE FLIGHT CENTER  
Greenbelt, Maryland

# THE GLOBAL RADIATION BALANCE OF THE EARTH ATMOSPHERE SYSTEM OBTAINED FROM RADIATION DATA OF THE METEOROLOGICAL SATELLITE NIMBUS II

Ehrhard Raschke\* and Musa Pasternak  
Laboratory for Atmospheric and Biological Sciences

## ABSTRACT

The meteorological satellite Nimbus II measured the reflected solar radiation in the spectral range from 0.2 to 4.0 microns and the emitted thermal radiation in the spectral range from 5.0 to 30.0 microns over the entire globe during a period of about 2.5 months (16 May - 28 July, 1966). These measurements were obtained with a medium resolution scanning radiometer. Thus, to compute the outgoing fluxes of reflected solar radiation and of emitted thermal radiation, empirical integration methods had to be applied to the measured data. For the computation of the emitted thermal radiation a method previously developed by Wark et al. [23] was used. Functional relations were derived from balloon, airplane, and satellite measurements of reflected solar radiation to account for the angular dependence of the reflectivity of the earth-atmosphere system in calculating the flux of reflected solar radiation. Results were obtained for five subperiods each of half a month's duration.

In this paper global maps are presented and discussed showing the geographic distribution of the albedo, the absorbed solar radiation, the emitted thermal radiation, and the radiation balance, obtained from the Nimbus II measurements during the subperiod 1 - 15 June, 1966. All other results are discussed elsewhere [18].

The global average of the radiation balance for all five subperiods was between  $-0.007$  and  $+0.002$   $\text{cal cm}^{-2} \text{ min}^{-1}$  indicating that the earth-atmosphere system is nearly in radiative equilibrium. These values are, however, within the limits of uncertainty of the computed fluxes of incoming and reflected solar radiation and the thermal radiation. The global average of the albedo was found to be about 30%, suggesting that other authors who found a value of about 35% from climatological data might have overestimated the cloudiness, especially in tropical latitudes.

---

\*On leave from the University of Munich as a Postdoctoral Resident Research Associate of the National Academy of Sciences.

# CONTENTS

	<u>Page</u>
INTRODUCTION . . . . .	1
METHODS OF COMPUTATION . . . . .	3
DISCUSSION OF THE RESULTS . . . . .	6
Albedo and Absorbed Solar Radiation . . . . .	6
Outgoing Longwave Radiation . . . . .	7
Radiation Balance $Q$ . . . . .	8
REFERENCES . . . . .	18

## TABLES

### Table

1	24-Hour Average of the Incoming Flux of Solar Radiation (S) During the Period 1 - 15 June 1966 at Given Latitudes. Values in $\text{cal cm}^{-2} \text{min}^{-1}$ . . . . .	7
2	Global Radiation Balance from Nimbus II Measurements . .	9
3	Radiation Balance of the Earth-Atmosphere System Over the Northern Hemisphere . . . . .	10

## ILLUSTRATIONS

<u>Figure</u>	<u>Page</u>
1     Radiance ( $N_f$ ) of emitted thermal radiation in the filter range from 5.0 to 30.0 microns vs the total radiance ( $N$ ) in the entire spectrum. Both quantities are given here in units of the radiant emittance ( $= \pi \cdot N$ ) . . . . .	11
2     The relative change of the total reflectance, $r$ , of the earth-atmosphere system with the sun's zenith angle, $\zeta$ . . . . .	12
3     The albedo of the earth-atmosphere system during the period 1 - 15 June, 1966. Values in % . . . . .	13
4     Solar radiation absorbed daily in the earth-atmosphere system during the period 1 - 15 June, 1966 . . . . .	14
5     Thermal radiation emitted daily from the earth-atmosphere system to space during the period 1 - 15 June, 1966 . . . . .	15
6     Radiation balance of the earth-atmosphere system during the period 1 - 15 June, 1966 . . . . .	16
7     Zonal averages of the radiation balance of the earth-atmosphere system . . . . .	17

THE GLOBAL RADIATION BALANCE OF THE EARTH  
ATMOSPHERE SYSTEM OBTAINED FROM RADIATION  
DATA OF THE METEOROLOGICAL  
SATELLITE NIMBUS II

## INTRODUCTION

The earth-atmosphere system both receives energy from and loses energy into space by radiation. Solar electromagnetic radiation in the spectral range from 0.1 - 4.0 microns forms the major energy source. About 60 - 70% of it is absorbed in atmospheric layers below about 150 - 200 km and at the ground. The rest is reflected and scattered back to space. Solar particle radiation influences highly the properties of atmospheric layers above 200 - 250 km. Its contribution to the total radiation influx and also the contribution of radiation from other extraterrestrial sources, however, is small enough to be neglected in these considerations. Energy is lost to space by emission of thermal radiation from ground and cloud surfaces and from several atmospheric gases. The main energy transfer by thermal radiation takes place in the spectral range from 5 to 50 microns.

The absorption and reflection (and scattering) of incident solar radiation and the emission of thermal radiation are primarily effective at the ground and in the lower atmosphere up to about 40 km. Very shortwave solar radiation at wavelengths less than 0.3 microns is absorbed in upper atmospheric layers, where it is responsible for many processes. It only amounts to about 1.5% of the total incoming radiation flux. Thus the radiation balance  $Q$  at the top of the atmosphere, which is the difference between incoming and outgoing radiation, determines in the first order the radiation balance of the earth-atmosphere system below the 40 km level. It can be expressed by:

$$Q(\lambda, \phi, d) = S(\lambda, \phi, d) - R(\lambda, \phi, d) - E(\lambda, \phi, d) \quad (1)$$

In Eq. (1)  $S$ ,  $R$ , and  $E$  are the fluxes of incoming and reflected solar radiation and of the emitted thermal radiation, respectively, crossing a horizontal element of area outside the atmosphere, whose geographic longitude and latitude are  $\lambda$  and  $\phi$  respectively. The letter  $d$  designates the day of the year for which the balance computations are made, during which the sun has a certain declination and distance from the earth.

Earlier computations of  $Q$  (e.g. see ref. [5], [10], [14]) were made with climatological data of various atmospheric parameters. All of these studies concluded that in general there is an excess of incoming radiation at low

latitudes and a deficit at high latitudes, the amplitude and location of which change with the seasons. This causes an energy transport by the general circulation in the atmosphere and by ocean currents. The yearly global average was found to be zero, suggesting that the earth-atmosphere system is in energy equilibrium over a period of a number of years.

These computations, however, were based on observational material whose reliability especially over polar regions and over oceanic areas at that time was much in doubt. Therefore, satellite experiments were designed to measure the fluxes of reflected solar radiation and of emitted longwave radiation over the entire earth. Prior to the Nimbus II medium resolution radiation experiment, radiation experiments were flown on Tiros satellites which observed only parts of the earth's surface between about  $60^{\circ}\text{N}$  and  $60^{\circ}\text{S}$ . Results obtained from these measurements (e.g. see ref. [3], [11], [19]) only confirmed the magnitude of the earlier computed values of the outgoing longwave radiation. The outgoing flux of reflected and scattered solar radiation was computed from the satellite data assuming isotropy of the reflection properties of surfaces and the atmosphere above them (Lambert surface). The results so obtained were too low to balance on a global scale the incoming solar radiation (S) with the outgoing radiation fluxes (R and E). Since there was no calibration on board the satellite, it was suspected that the instruments suffered a degradation in their response. Based on this and on the assumption of an annual global radiation balance  $Q = 0$ , Bandeen et al. [3] derived correction factors with which the satellite measurements of outgoing solar radiation were multiplied to determine the total outgoing flux of solar radiation from satellite measurements. Rasool and Prabhakara [19] and Arking [1] have treated Tiros radiation data in a similar way.

Theoretical computations (e.g. see ref. [7], [9]) as well as some measurements from balloons or airplanes ([4], [6], [21]) however, indicate a predominant dependence of the reflection properties of surfaces and of the atmosphere above on the zenith angle and azimuth angle (with respect to the sun) of observation, and also on the elevation of the sun above the horizon. Arking [1] confirmed these findings with a statistical analysis of Tiros IV measurements of the reflected solar radiation in the spectral interval from 0.2 - 4.0 microns.

Thus, it is suggested, that the assumption of a Lambert-surface for calculations of the outgoing reflected flux of solar radiation is the reason for the apparently low results. As a consequence, for the computations of the outgoing flux of solar radiation from Nimbus II measurements efforts have been made to take into account the angular dependence of the reflection properties of the earth-atmosphere system.

The medium resolution radiometer in Nimbus II provided measurements of the emitted longwave radiation and reflected solar radiation over the entire



globe during a period of about 2.5 months (16 May - 28 July, 1966). This period covers the beginning and development of the summer and winter seasons in the Northern and Southern hemispheres, respectively. But it is too short, to draw any conclusions about the annual radiation balance.

This entire period was divided into five subperiods, each of half a month's duration, for which global distributions of S, R, E, and Q (Eq. 1) and some related quantities were computed. In this paper only results which were obtained from the Nimbus II measurements of the period 1 June - 15 June, 1966 are presented and discussed. All other results are presented in more detail in a comprehensive report on this project [18].

## METHODS OF COMPUTATION

Nimbus II was launched on May 15, 1966 into a sunsynchronous, nearly polar and circular orbit. At a mean height of 1140 km above the surface of the earth, it crossed the equator in the northward direction at around local noon and in the southward direction at around local midnight. Due to its orbital period of 107 minutes and due to its height, generally each area element on the earth was observed at least once in the daytime and once in the nighttime within a 24 hour interval. Thus within 24 hours reflected solar radiation was observed at least once over each area of the illuminated portion of the earth. Emitted long-wave radiation could be measured from the same area both during day and night. The Nimbus II experiment is described in more detail elsewhere [17].

Two channels of the five-channel medium resolution radiometer were designed to measure the reflected solar radiation (0.2 - 4.0 microns) and the emitted longwave radiation (5.0 - 30.0 microns). The instantaneous angular field of view of the radiometer subtends an overall angle of about 4 degrees. Therefore, the computation of both fluxes through an area outside the atmosphere, which is perpendicular to the earth's radius vector through it, would require measurements from all directions to perform the integration over the entire hemisphere, as expressed mathematically by:

$$\text{Flux} = \int_0^{2\pi} \int_0^{\pi/2} N(\theta, \psi) \sin \theta \cos \theta \, d\theta \, d\psi \quad (2)$$

In Eq. 2  $\theta$  is the zenith angle of observation at the observed area,  $\psi$  is the azimuth counted from a fixed position (e.g. the horizontal projection of the solar ray incident upon the observed point), and  $N(\theta, \psi)$  stands for the total radiance of reflected sunlight or of emitted thermal radiation determined from the satellite measurements.

An integration according to Eq. (2) at the height of the satellite would cause a great loss of detail in all measured radiation fields (e.g., see [15]). Therefore, it was assumed here, that the reference level is located on the surface of a spherical earth with a radius of 6371 km. This includes the assumption that this surface has the same physical properties (reflection, scattering, refraction, emission) as the earth-atmosphere system. Now the outgoing fluxes of reflected solar radiation (R) and of emitted longwave radiation (E) were considered to be radiation fluxes from an element of area into the upward hemisphere above it. The geographic coordinates of this element of area are determined from a knowledge of the motion of the spacecraft in orbit and of the phase of the scanner mirror in the reduction of the original analog signals. The computation methods are only very briefly outlined here; they are discussed in more detail elsewhere [18].

The outgoing flux of emitted longwave radiation has been computed by the method of Wark et al. [23]. This method consists of two major steps:

1. From the radiance measured in the spectral range from 5.0 to 30.0 micron, the radiance over the entire spectrum is computed. For this a relation between both quantities has been derived from computations of both the "filtered" and "unfiltered" radiance emerging from a set of more than 100 atmospheric profiles into different directions ( $\theta$ ). Some results of these computations, which were carried out by Lienesch [13], are presented as points ( $\theta = 0$ ) and as encircled points ( $\theta = 78.5^\circ$ ) in Fig. 1. These points approach narrowly a straight line because the range of sensitivity of the filter (5.0 - 30.0 microns) covers that spectral region within which about 90% of the totally emitted longwave radiation emerges to space.

2. The second step includes the integration of radiances emitted into all directions. Here only the dependence on the zenith angle  $\theta$  was taken into account by a function obtained statistically from Tiros VII measurements [13]. No dependence of N was assumed with respect to the azimuth angle. To obtain a representative average of longwave radiation emitted during a 24 hour interval, the results from daytime and nighttime measurements were averaged, weighting each with the length of day and of night, respectively.

The outgoing flux of reflected and scattered solar radiation also was computed as an average for a 24 hour interval. The method used here consists of 3 steps:

1. Due to its narrow field of view, the radiometer in Nimbus II measured only that portion  $\rho$  of solar radiation incident on an observed area which is reflected into the direction of the satellite. It is related to the measured radiance

$N_f(\theta, \psi)$  and to the solar radiation  $S_f(d)$  incident in the same filter range ( $\theta$ ) by

$$\rho(\theta, \psi, \zeta') = \frac{N_f(\theta, \psi)}{\cos \zeta' \cdot S_f(d)} \quad (\text{sr}^{-1}) \quad (3)$$

Here  $\zeta'$  is the zenith angle of the sun at time of measurement, and  $d$  expresses the day of measurement as described in the introduction above.  $S_f$  has been obtained by integrating over all wavelengths the product of the spectral response of the instrument with Johnson's [12] data on the extraterrestrial spectral solar irradiance. Since the spectral response of the instrument covers that range, within which about 99% of the energy of solar radiation enters the atmosphere, it is assumed in all further steps, that  $\rho$  is a mean value for the entire solar spectrum.

2.  $\rho$  is only the reflectance into one direction. The total reflectance  $r$  ( $\rho$ ) is the ratio between the total reflected and scattered solar radiation in the upward hemisphere and the incident solar radiation. The functional relationship  $r$  ( $\rho$ ) has been determined using conversion factors which were derived from many measurements of the angular dependence of the reflected solar radiation made from airplanes and balloons ([4], [6], [21]) and from Arking's [2] statistical analyses of Tiros IV measurements. (For a Lambert surface  $r = \pi \cdot \zeta$ .)

3. In general, the  $r$  of an area element over a given underlying surface depends strongly on the zenith angle of the sun  $\zeta$ . However, the functional relationship between  $r$  and  $\zeta$  also depends upon the nature of the underlying surface, the turbidity of the air, etc. In these calculations only one function describing the dependence of  $r$  on the sun's zenith angle has been used. It was derived from the measurements and analyses mentioned above. Figure 2 compares our function with results by Arking and Levine, showing a general increase of total reflectance of the earth-atmosphere system as the sun approaches the horizon. In this third step the total reflectance  $r$  was computed for all other zenith angles of the sun which are possible between sunrise and sunset over a certain area.

The fluxes of incoming and of outgoing solar radiation were computed on the basis of the currently accepted value of the solar constant:  $S_0 = 2.0 \text{ cal cm}^{-2} \text{ min}^{-1}$ . Corrections were applied for the actual earth-sun distance on a given day  $d$  and for the effects of refraction, based upon a standard atmosphere.

The use of the above mentioned generalized functional relations undoubtedly causes errors where these functions do not coincide with the actual conditions. But, it is assumed that these errors are kept within an acceptable limit averaging all single measurements of a longer time interval within larger areas.

Therefore, a standardized grid program was used in which all single measurements are averaged within fields of the size of about 5 degrees of longitude and 2 to 5 degrees of latitude.

## DISCUSSION OF THE RESULTS

### Albedo and Absorbed Solar Radiation

The albedo  $A$  of an area is defined here as that part of the daily incoming flux of solar radiation which is reflected back to space:

$$A(\lambda, \phi, d) = \frac{R(\lambda, \phi, d)}{S(\lambda, \phi, d)} \cdot 100 [\%] \quad (4)$$

It is characteristic for the reflection properties of the earth-atmosphere system at this area and determines the absorbed (ABS) part of the incoming flux by:

$$ABS(\lambda, \phi, d) = \left( 1 - \frac{A(\lambda, \phi, d)}{100} \right) \cdot S(\lambda, \phi, d) \quad (5a)$$

$$= S(\lambda, \phi, d) - R(\lambda, \phi, d) \quad (5b)$$

Global maps of these quantities are shown in Figs. 3 and 4.

It is known from other investigations that clouds, ice and snow surfaces are very good reflectors of incoming solar radiation. Therefore, the high albedoes in Fig. 3 can be interpreted to be caused either by clouds and/or by snow and ice surfaces. Cloud fields associated with the Intertropical Convergence Zone, the Monsoon over Southeast Asia, and the polar frontal zones of both hemispheres cause albedoes of more than 40%. Over the ice and snow covered polar cap north of 70° N, 60-80% of the incident radiation is reflected back to space. The reflectance of the surfaces here is increased by the low elevation of the sun throughout the entire day (Fig. 2). The desert areas of North Africa, Arabia and also of Australia exhibit albedoes of more than 30-40%.

Water surfaces have albedoes of less than 10%. Therefore, over the less cloud-covered subtropical oceans only 10-20% of the incident solar radiation is lost by reflection. The higher values for the albedoes of latitudes north of 50° N and south of 40° S indicate increased cloudiness. The general pattern of the albedo field in Fig. 3 and consequently of the field of absorbed solar radiation (Fig. 4) shows many irregularities over the Northern Hemisphere, due to the different influences of sea and land surfaces on the circulation and therefore on

the reflection properties of the earth-atmosphere system. The preponderance of water in the Southern Hemisphere causes a more zonal pattern which is even more pronounced in the field of absorbed solar radiation (Fig. 4), due to the strong meridional gradient of incident solar radiation at these latitudes. Since measurements obtained at solar zenith angles  $\zeta'$  of more than  $80^\circ$  were omitted, both fields show no data south of  $58^\circ\text{S}$ . The polar cap south of  $68^\circ\text{S}$  was not illuminated by the sun at this time of the year.

Table 1  
24-Hour Average of the Incoming Flux of Solar Radiation (S)  
During the Period 1 - 15 June 1966 at Given Latitudes.  
Values in  $\text{cal cm}^{-2} \text{ min}^{-1}$ .

	North					South				
Latitude:	$90^\circ$	$80^\circ$	$60^\circ$	$40^\circ$	$20^\circ$	$0^\circ$	$20^\circ$	$40^\circ$	$60^\circ$	$68^\circ$
Flux:	0.75	0.74	0.69	0.71	0.67	0.57	0.41	0.22	0.06	0

If the albedo of the Northern Hemisphere were uniform, the North Pole would daily absorb during this time of the year even more solar energy than the subtropics (Table 1). The geographic distribution of the albedoes, however, causes a maximum of solar radiation of more than  $0.54 \text{ cal cm}^{-2} \text{ min}^{-1}$  to be absorbed over a latitude belt between about  $10^\circ$  and  $35^\circ\text{N}$  (Fig. 4). This belt is interrupted over North Africa and Arabia, and Southeast Asia where deserts and clouds, respectively, cause a high albedo. From this belt the amount of absorbed solar radiation decreases toward both poles more or less continuously, due primarily to the increase of albedo (northward) and the decrease of the incoming flux (southward).

In general meridional profiles of the absorbed solar radiation show that over the oceans more radiation is absorbed than over land at the same latitude.

#### Outgoing Longwave Radiation

The absorption spectrum of the earth's atmosphere has a wide window between 8 and 13 microns, through which radiation emitted from ground or cloud surfaces penetrates to space only weakly influenced by absorption and emission in intervening atmospheric layers. In this part of the spectrum also Planck's function of the spectral radiance of thermal radiation has its maximum for temperatures between  $230^\circ\text{K}$  and  $300^\circ\text{K}$  normally occurring in the atmosphere and at the ground. Therefore, the outgoing flux of longwave radiation can be considered to be in first order a function of the temperature of the underlying

surface. This surface might be a cloud, land, or ocean. This interpretation seems to be confirmed by a high correlation between simultaneous measurements of the upward going radiation in the spectral intervals 8 - 13 microns and 7.5 - 32.5 microns, found by Möller and Raschke [16] from radiation data of the satellite Tiros III. Linear correlation coefficients of between 0.85 and 0.95 were found for data of different orbits. Thus the pattern of the outgoing long-wave radiation as shown in Fig. 5 can be interpreted in terms of the temperature of underlying cloud, land, or ocean surfaces. Pronounced minima of outgoing longwave radiation have been found over both polar caps, especially over the Plateau of Queen Maud Land. Very high and cold cloud fields associated with the intertropical convergence zone and with the monsoon over Southeast Asia occur in Fig. 4 as minima at low latitudes. The emitted flux is high over the sparsely cloud covered areas of the subtropical oceans and over the warm land surfaces at the same latitudes.

### Radiation Balance Q

The net radiation flux at the top of the atmosphere or the radiation balance of the earth-atmosphere system can be found by subtracting the outgoing long-wave radiation of each area from the corresponding value of absorbed solar radiation. Figure 6 shows the geographic distribution found for the period 1 - 15 June, 1966.

These results show that all over the globe between 10° S and about 70° N the absorbed solar radiation exceeds the emitted longwave radiation. This leads to a surplus of energy which is partly stored in the oceans, ground, and atmosphere, and partly transported by the general circulation and by ocean currents into regions of radiation deficit. Maxima of radiation excess are found over the subtropical oceans, while the hot deserts in the same latitudes show even a slight radiation deficit. This result is in good agreement with the work of Budyko [5] which showed an annual radiation deficit over the same regions.

The highest radiation deficit of the Northern Hemisphere was found over Greenland, where only about 20-25% of incoming solar radiation is absorbed.

At southern latitudes between 55° and 70° deficits of more than 0.24 cal cm<sup>-2</sup> min<sup>-1</sup> result from relatively high surface temperatures of ice and probably open water and from the very low amount of incoming solar radiation. Since at this time of year the South Pole, especially the Plateau of Queen Maud Land, has very low surface temperatures of about 205° K, it shows a lower radiation deficit than the ice belt north of it.

Meridional profiles of zonal averages of Q obtained from these computations and from the results of other authors are compared in Fig. 7. They show, that

the other authors predicted in their results very similar meridional profiles, but found lower values for the radiation excess between 0° and 30° N. This is probably caused by higher values of the albedo found by these authors over these latitudes (e.g., London 31 - 34% vs Nimbus II 22 - 27%). The global average of the radiation balance (Table 2) was found for all five subperiods to be between +0.002 and -0.007 cal cm<sup>-2</sup> min<sup>-1</sup>, confirming that the earth atmosphere system is close to a radiation balance. These values, however, are differences between two very large numbers, the globally absorbed solar radiation and emitted longwave radiation, and are within the uncertainties of those large numbers. Thus, no final conclusion on a net heating or cooling of the entire system during each of these subperiods can be drawn from these values.

Table 2  
Global Radiation Balance from Nimbus II Measurements

	Albedo %	Absorbed Solar Radiation cal cm <sup>-2</sup> min <sup>-1</sup>	Outgoing Longwave Radiation cal cm <sup>-2</sup> min <sup>-1</sup>	Radiation Balance cal cm <sup>-2</sup> min <sup>-1</sup>
May 16-31	30.1	0.341	0.339	+0.002
June 1-15	30.6	0.337	0.342	-0.005
June 16-30	30.1	0.338	0.345	-0.007
July 1-15	29.1	0.343	0.346	-0.003
July 16-28	29.5	0.342	0.345	-0.003

In Table 2 the values obtained for the global albedo are also listed. Ranging from 29.1 to 30.6%, they are all lower than earlier estimates of the annual planetary albedo, which were found to be around 35% (e.g., see ref. [8]). Direct comparisons of results obtained from the Nimbus II measurements with earlier estimates obtained from climatological data are only possible for the Northern Hemisphere, for which London [14] computed the radiation balance and some related quantities, for the summer season (June-August). This comparison is given in Table 3.

The albedo value found by London is higher than those obtained from the Nimbus II measurements. Conversely, the total outgoing flux of longwave radiation as determined by London is lower than those obtained from the Nimbus II measurements.

Clouds influence both the albedo and the outgoing longwave radiation. From the consideration made above, it might be suspected that surface observations

used by London may have overestimated the low latitude cloudiness, thus producing too high values of the albedo and too low values of the outgoing flux of longwave radiation.

Table 3  
Radiation Balance of the Earth-Atmosphere  
System Over the Northern Hemisphere

		Albedo %	Absorbed Solar Radiation cal cm <sup>-2</sup> min <sup>-1</sup>	Outgoing Longwave Radiation cal cm <sup>-2</sup> min <sup>-1</sup>	Radiation Balance cal cm <sup>-2</sup> min <sup>-1</sup>
London	June-July- August	36.3	0.411	0.339	+0.072
Nimbus II	May 16-31	32.8	0.443	0.345	+0.098
	June 1-15	32.8	0.452	0.349	+0.103
	June 16-30	32.2	0.458	0.353	+0.105
	July 1-15	31.5	0.458	0.355	+0.103
	July 16-28	30.9	0.446	0.355	+0.091



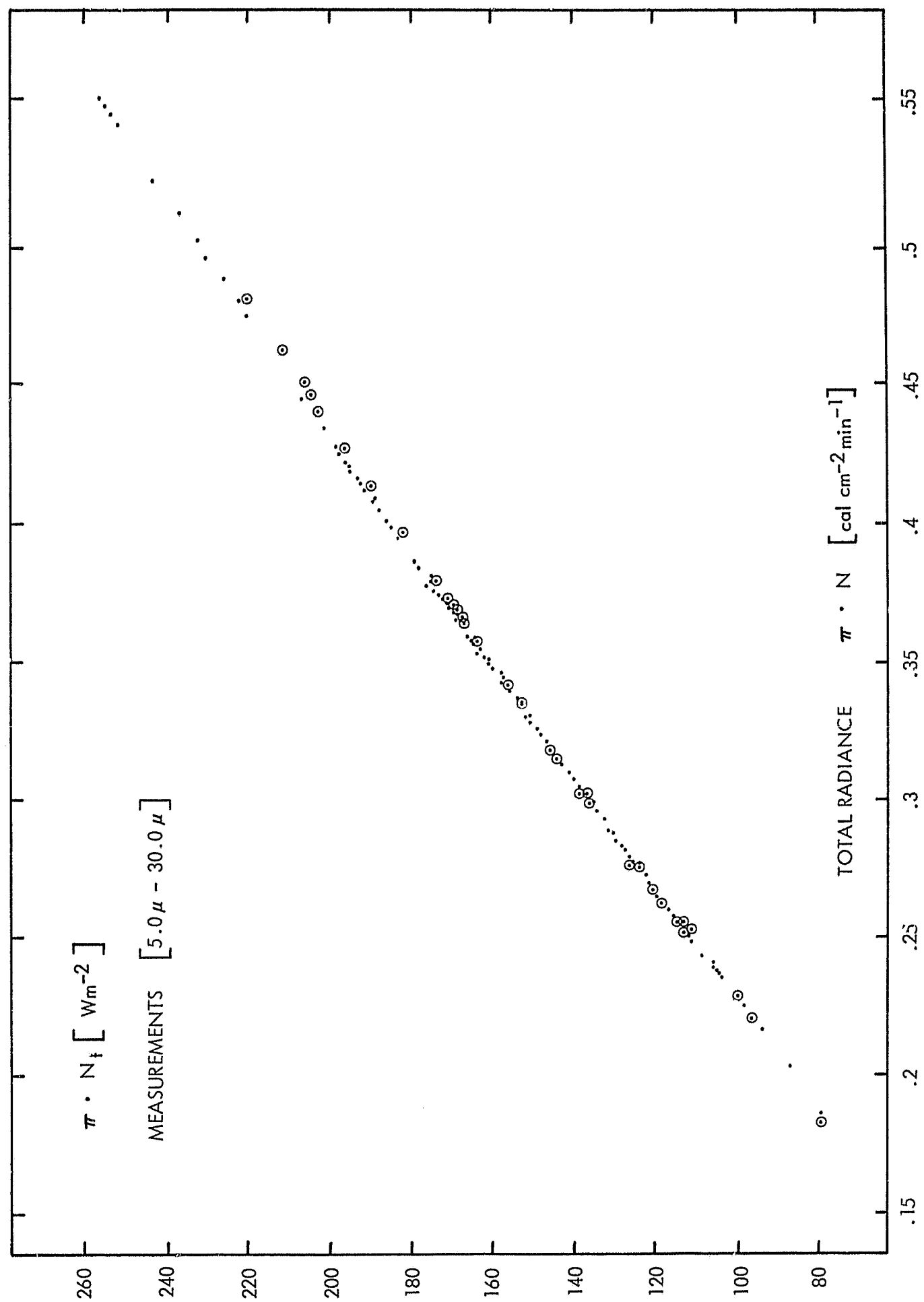


Figure 1. Radiance ( $N_f$ ) of emitted thermal radiation in the filter range from 5.0 to 30.0 microns vs the total radiance ( $N$ ) in the entire spectrum. Both quantities are given here in units of the radiant emittance ( $= \pi \cdot N$ ).

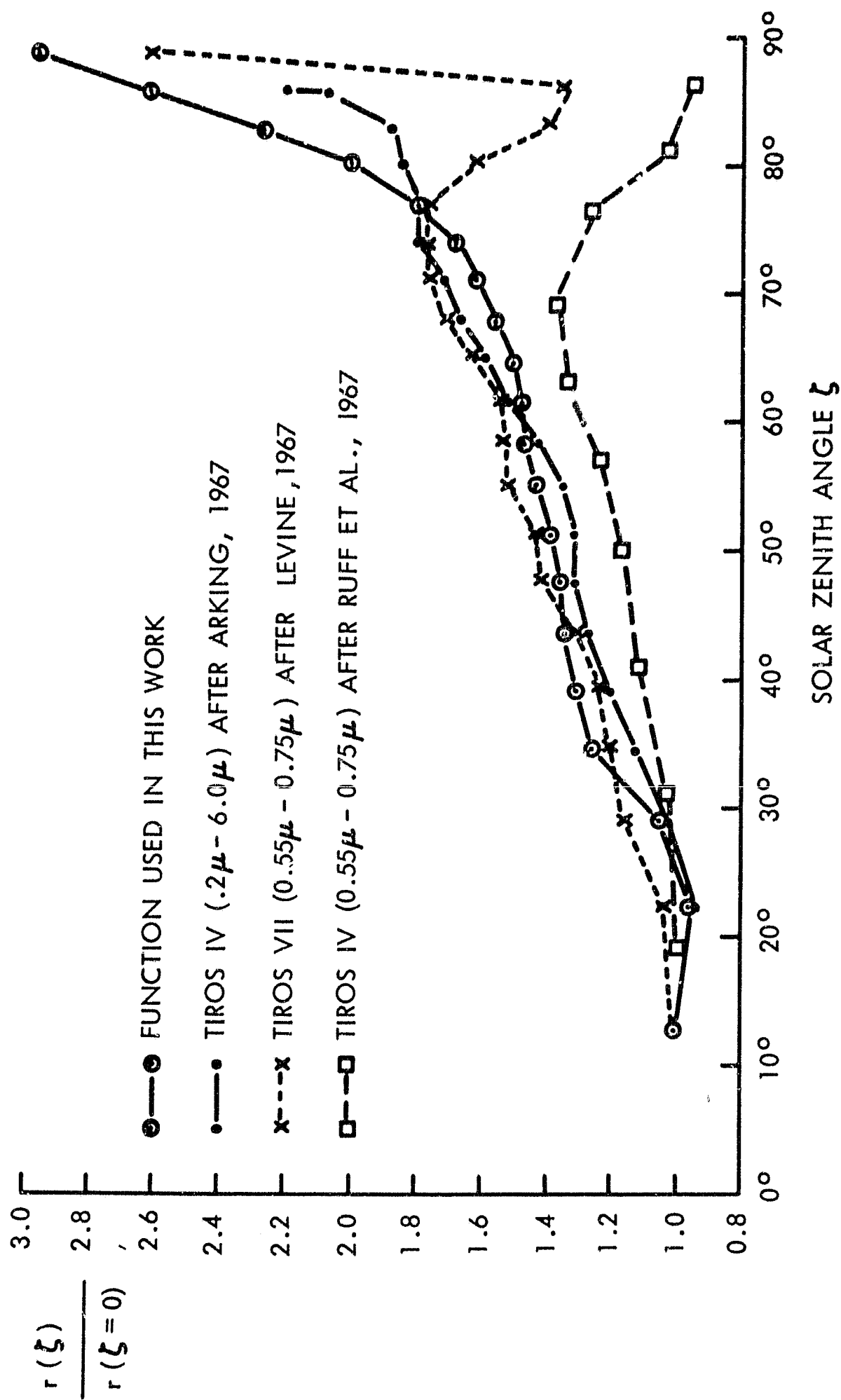


Figure 2. The relative change of the total reflectance,  $r$ , of the earth atmosphere system with the sun's zenith angle,  $\zeta$ .

ALBEDO [%]  
NIMBUS II 1 - 15 JUNE 1966

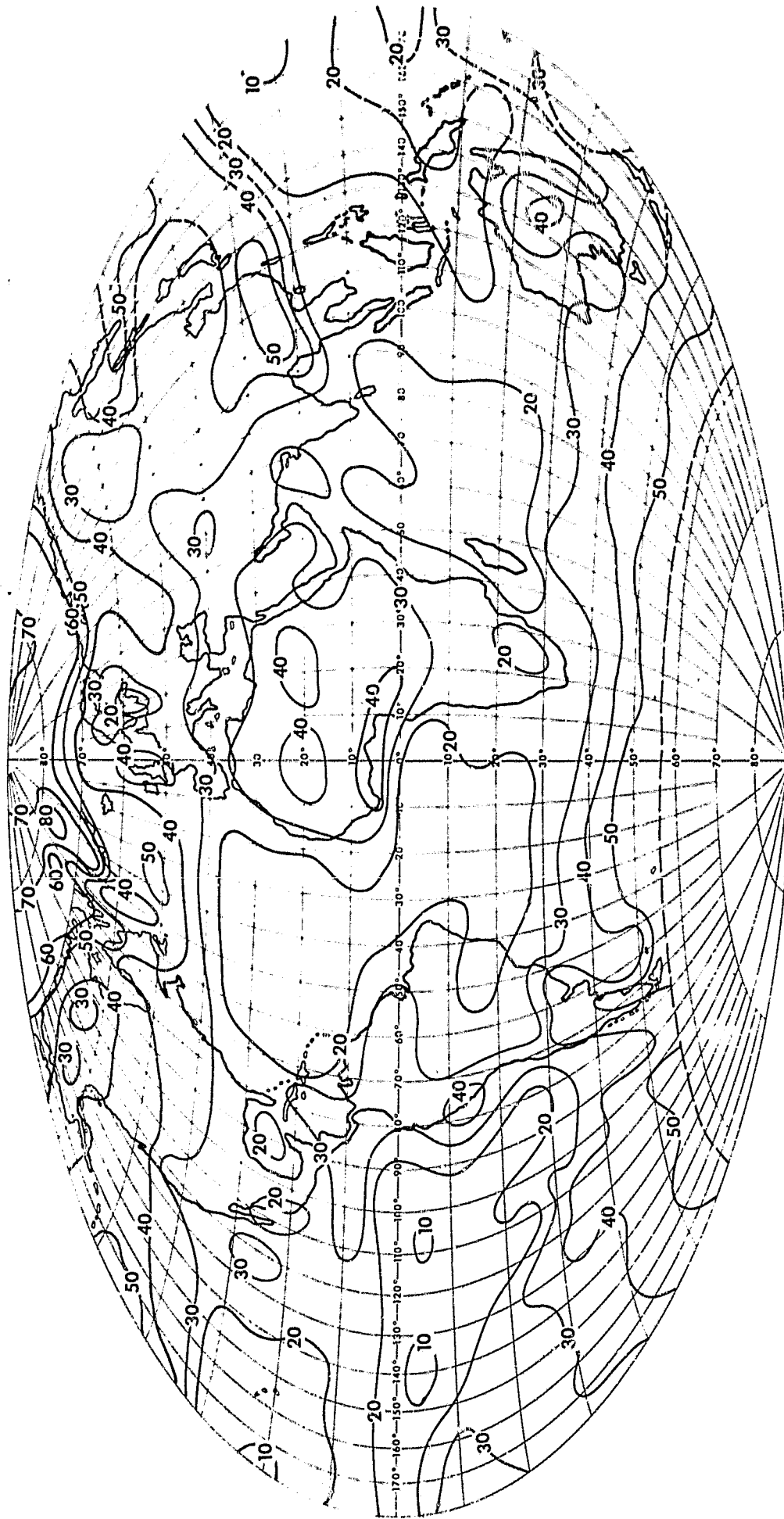


Figure 3. The albedo of the earth-atmosphere system during the period 1 - 15 June, 1966. Values in %.

ABSORBED SOLAR RADIATION [ $\text{LY MIN}^{-1}$ ]  
NIMBUS II 1 - 15 JUNE 1966

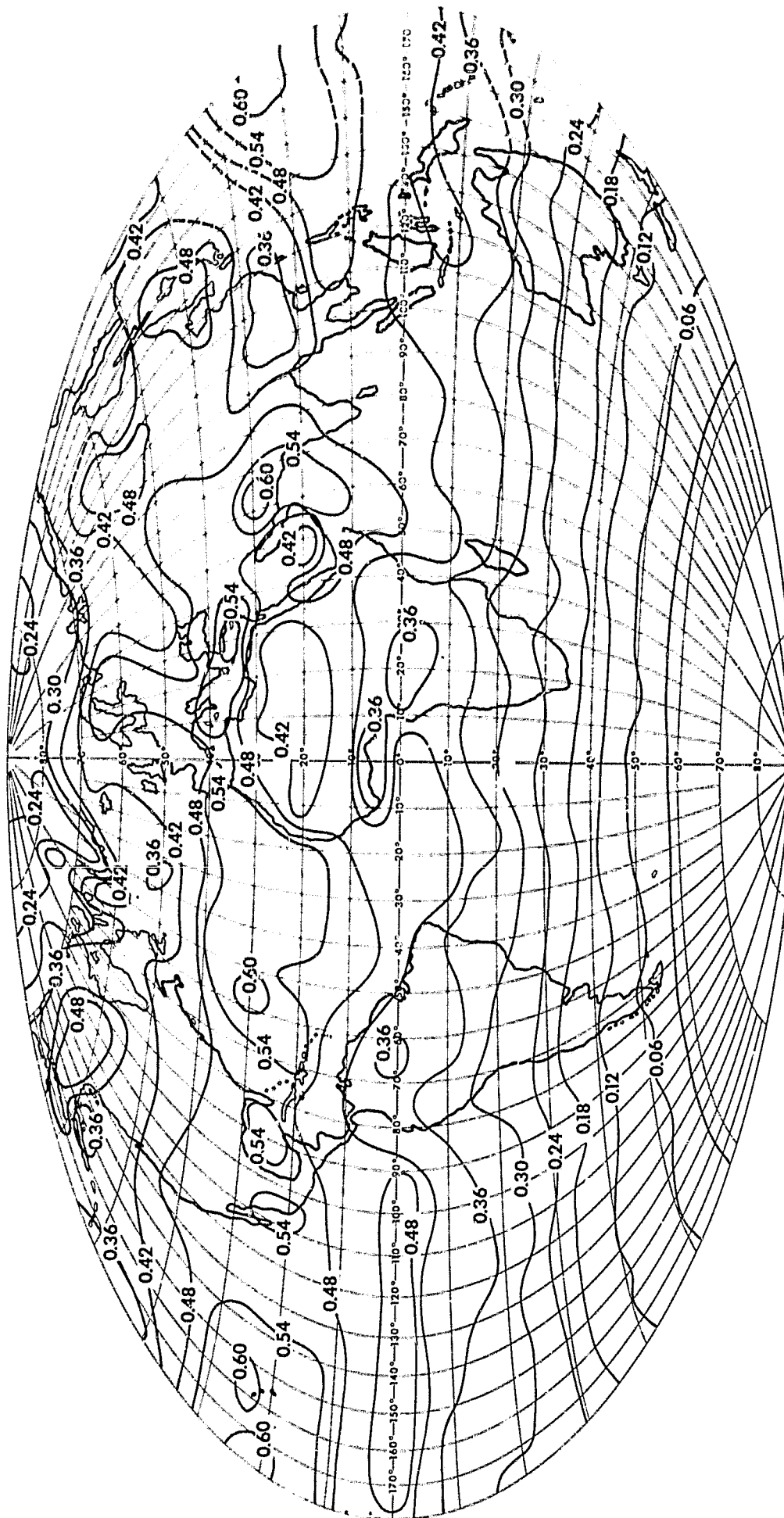


Figure 4. Solar radiation absorbed daily in the earth-atmosphere system during the period 1 - 15 June, 1966.

OUTGOING TOTAL LONGWAVE RADIATION [ $\text{LY MIN}^{-1}$ ]  
 NIMBUS II 1 - 15 JUNE 1966

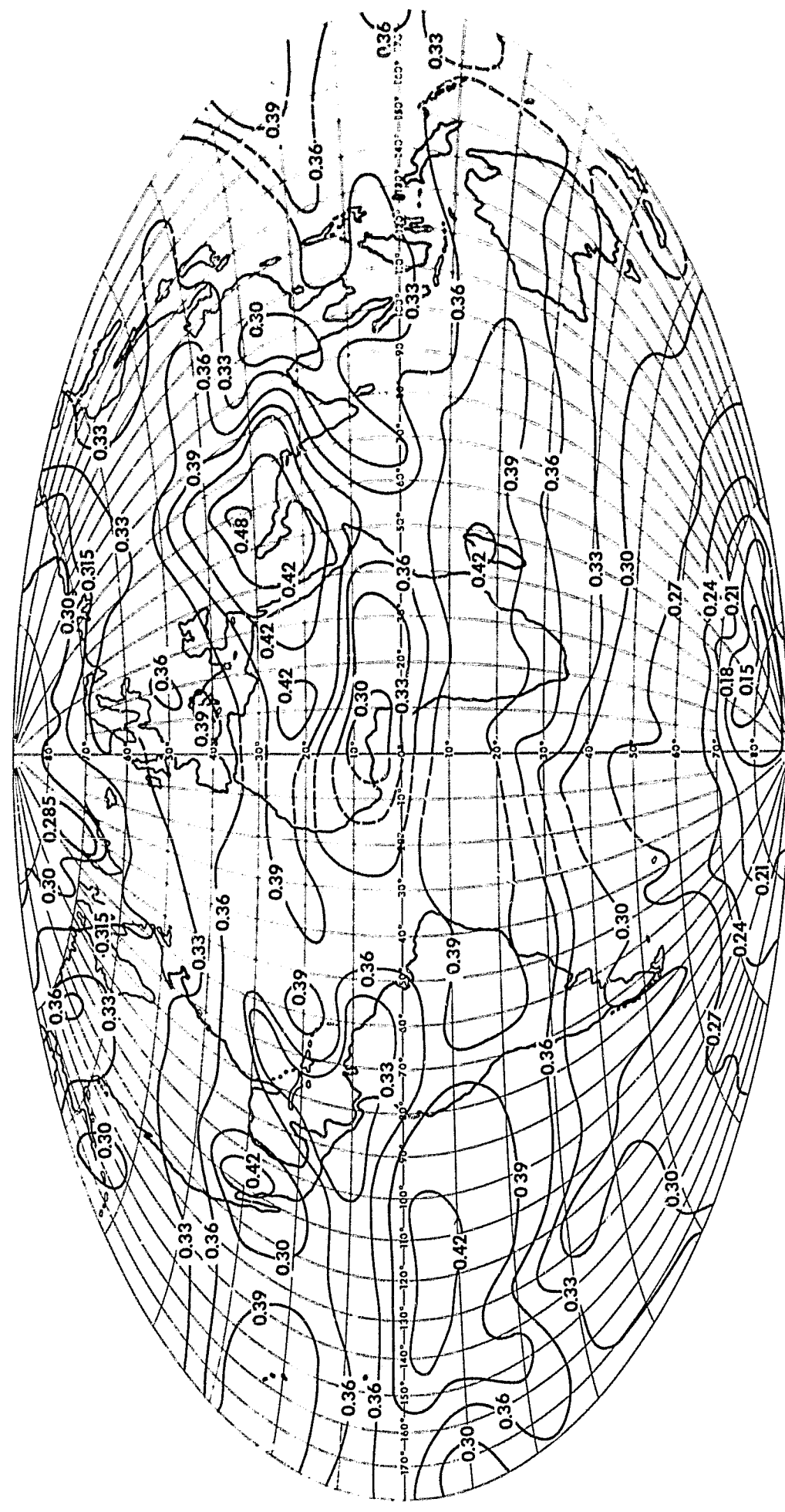


Figure 5. Thermal radiation emitted daily from the earth-atmosphere system to space during the period 1 - 15 June, 1966.

NET RADIATION FLUX AT THE TOP OF THE ATMOSPHERE [ $\text{LY MIN}^{-1}$ ]  
NIMBUS II 1 - 15 JUNE 1966

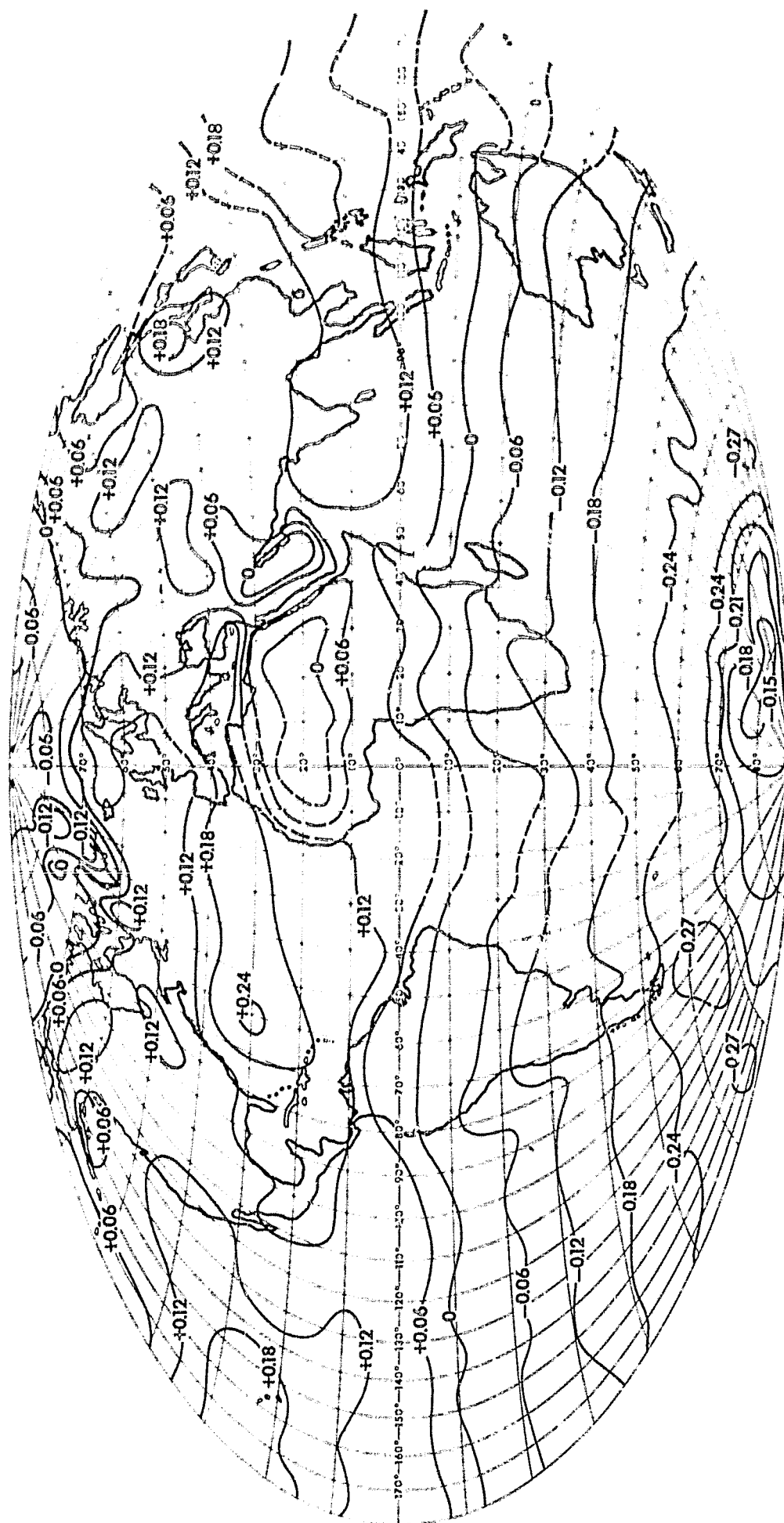


Figure 6. Radiation balance of the earth-atmosphere system during the period 1 - 15 June, 1966.

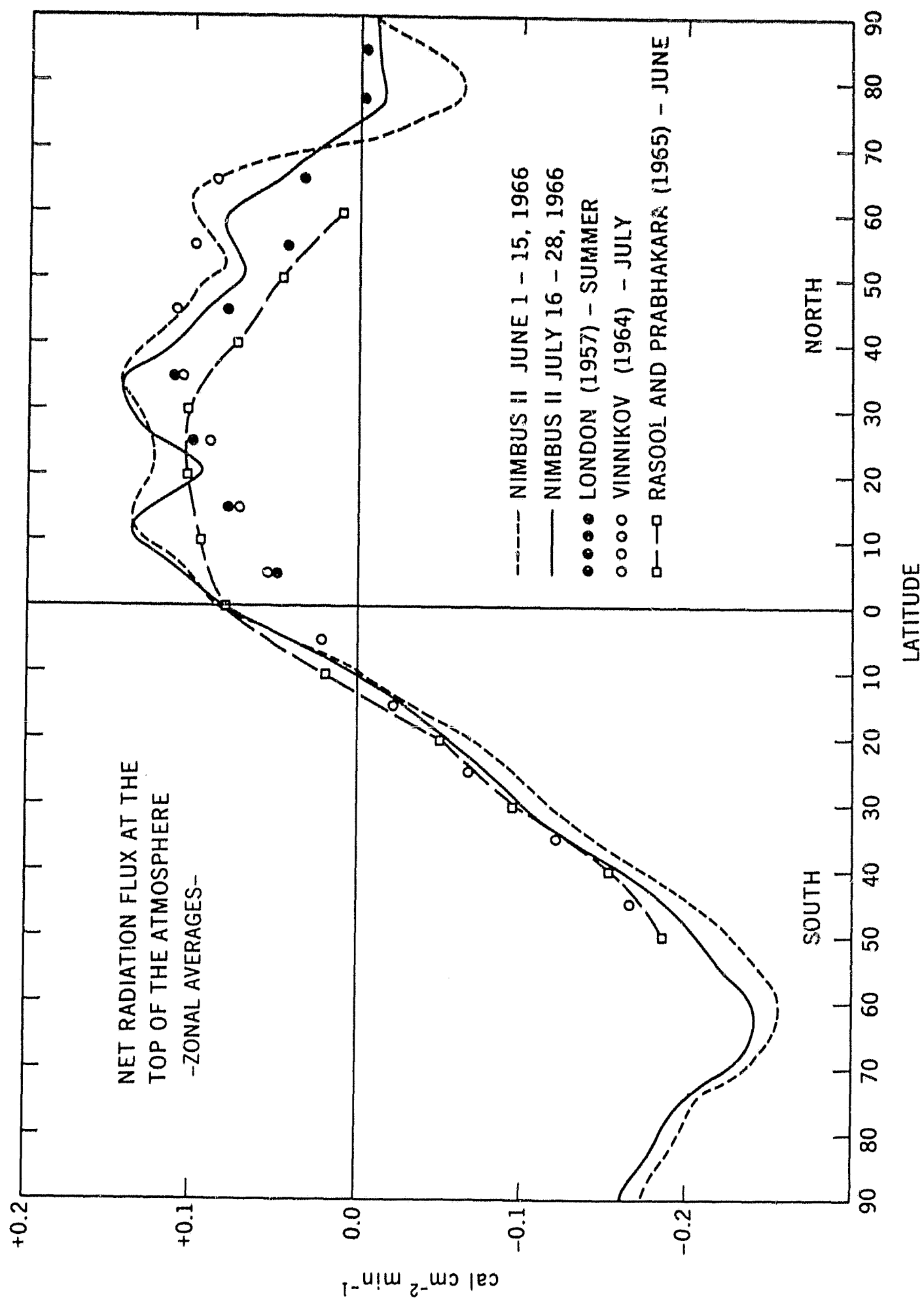


Figure 7. Zonal averages of the radiation balance of the earth-atmosphere system.

**BLANK PAGE**



## REFERENCES

1. Arking, A.: The Angular Distribution of Scattered Solar Radiation and the Earth Albedo as Observed from Tiros. Institute for Space Studies, New York, Research Reports, July 1, 1964 - June 30, 1965, pp. 47-67
2. Arking, A., and Levine, J.: Private Communications, not yet published, 1967
3. Bandeen, W. R., Halev. M., and Strange, I.: A Radiation Climatology in the Visible and Infrared from the Tiros Meteorological Satellites. NASA Technical Note D-2534, 1965
4. Bartman, F. L.: The Reflectance and Scattering of Solar Radiation by the Earth. Technical Report, 257 pp, University of Michigan, Contract No. NASr-54(03), 1967
5. Budyko, M. I., ed.: Atlas of the Heat Balance of the Earth (Atlas Teplovo-go Balansa Zemnogo Shara), Moscow, 1963
6. Cherrix, T., and Sparkman, B.: A Preliminary Report on Bidirectional Reflectances of Stratocumulus Clouds Measured with an Airborn Medium Resolution. NASA X-622-76-48, GSFC, 1965
7. Coulson, K. L.: Effects of Reflection Properties of Natural Surfaces on Aerial Reconnaissance. Appl. Optics, 5, 905-917, 1966
8. Fritz, S.: The Albedo of the Planet Earth and Clouds, Journ. Meteor, 6, 277-282, 1949
9. Heger, K.: Die von der getrübbten Atmosphäre nach außen gestreute Strahlung. Beiträge. z. Phys. d. Atm. 39, 12-36, 1966
10. Houghton, H. G.: On the Annual Heat Balance of the Northern Hemisphere. Journ. of Met., 11, 1-9, 1954
11. House, F. B.: The Radiation Balance of the Earth from a Satellite. Ph.D. Dissertation, University of Wisconsin, Department of Meteorology, 1965
12. Johnson, F. S.: Satellite Environment Handbook. Chapt. 4. Stanford University Press, Stanford, California, 95-105, 1966

13. Lienesch, F. H.: Private Communication, not yet published, 1966
14. London, J.: A Study of the Atmospheric Heat Balance. Final Report, Contract AF 19 (122) -165, Research Division, College of Engineering, 1957
15. London, J., Ooyama, K., and Viebrook, H.: Studies of Atmospheric Radiation as Observed from Satellites in "Contributions to Satellite Meteorology." Vol. II. Ed. by F. R. Valocin, AFCRL 438, GRD. Notes No. 36, Bedford, Mass., pp. 171-190, 1961
16. Möller, F., and Raschke, E.: Evaluation of Tiros III Radiation Data. NASA Contractor Report CR-112. (Grant NsG-305 with University of Munich), 1964
17. Nordberg, W., McCulloch, A. W., Foshee, L. L., and Bandeen, W. R.: Preliminary Results from Nimbus II. Bull. Am. Met. Soc., 47, 857-872, 1966
18. Raschke, E., and Pasternak, M.: The Extraterrestrial Radiation Balance from Measurements of the Meteorological Satellite Nimbus II. NASA Technical Report (in preparation), Goddard Space Flight Center, Greenbelt, Md., 1967
19. Rasool and Prabhakara: Radiation Studies from Meteorological Satellites. Geophysical Sciences Laboratory. Report No. 65-1, New York University, Department of Meteorology and Oceanography, 1965
20. Ruff, I., Koffler, R., Fritz, S., Winston, F. S., and Rao, P. K.: Angular Distribution of Solar Radiation Reflected from Clouds as Determined from Tiros IV Radiometer Measurements. ESSA Technical Report NESG-38, Washington, D. C., 1967
21. Salomonson, V.: Anisotropy of Reflected Solar Radiation from Various Surfaces as Measured with an Aircraft-Mounted Radiometer Research Report, Contract NASr-147, Colorado State University, 29 pp., 1966
22. Vinnikov, K. Y.: "The Heat Balance of the Earth," by M. I. Budyko and K. Y. Kondratiev. Research in Geophysics, Vol. 2, M.I.T. Press, 1964
23. Wark, D. Q., Yamamoto, G., and Lienesch, F. H.: Methods of Estimating Infrared Flux and Surface Temperature from Meteorological Satellites. J. Amer. Sci., 19, 369-384, 1962